

# Tin(II) Oxalates Synthesized in the Presence of Structure-Directing Organic Amines: Members of a Potentially Vast Class of New Open-Framework and Related Materials

S. Ayyappan,<sup>†</sup> Anthony K. Cheetham,<sup>\*,†</sup> Srinivasan Natarajan,<sup>‡</sup> and C.N.R. Rao<sup>\*,‡</sup>

Materials Research Laboratory, University of California, Santa Barbara, California 93106, and Chemistry and Physics of Materials Unit, Jawaharlal Nehru Centre for Advanced Scientific Research, Jakkur Campus, Jakkur P.O., Bangalore 560 064, India

Received August 18, 1998

Three new tin(II) oxalate materials, of which one has an open-framework layered structure, have been synthesized hydrothermally in the presence of structure-directing organic amines. Crystal data: oxalate **I**,  $[(\text{CH}_3)_2\text{NH}(\text{CH}_2)_4\text{NH}(\text{CH}_3)_2]^{2+}[\text{Sn}_2(\text{C}_2\text{O}_4)_3]^{2-}$ , monoclinic, space group  $P2_1/c$  (No. 14)  $a = 8.427(2) \text{ \AA}$ ,  $b = 14.257(1) \text{ \AA}$ ,  $c = 8.868(2) \text{ \AA}$ ,  $\beta = 100.3(1)^\circ$ ,  $V = 1048.3(2) \text{ \AA}^3$ ,  $Z = 4$ ,  $M = 738.6(1)$ ,  $D_{\text{calc}} = 2.06(1) \text{ g cm}^{-3}$ , Mo  $K\alpha$ ,  $R_{\text{F}} = 0.05$ ; oxalate **II**,  $[\text{C}(\text{NH}_2)_3]_2^+[\text{Sn}_2(\text{C}_2\text{O}_4)_3]^{2-} \cdot 2\text{H}_2\text{O}$ , triclinic, space group  $P\bar{1}$  (No. 2),  $a = 7.564(1) \text{ \AA}$ ,  $b = 10.633(1) \text{ \AA}$ ,  $c = 12.050(1) \text{ \AA}$ ,  $\alpha = 87.9(1)^\circ$ ,  $\beta = 85.2(1)^\circ$ ,  $\gamma = 85.9(1)^\circ$ ,  $V = 962.8(1) \text{ \AA}^3$ ,  $Z = 2$ ,  $M = 699.6(1)$ ,  $D_{\text{calc}} = 2.25(1) \text{ g cm}^{-3}$ , Mo  $K\alpha$ ,  $R_{\text{F}} = 0.06$ ; oxalate **III**,  $[\text{C}_5\text{N}_2\text{H}_{16}]^{2+}[\text{Sn}_2(\text{C}_2\text{O}_4)_3]^{2-}$ , orthorhombic, space group  $Pm\bar{m}n$  (No. 59),  $a = 8.281(2) \text{ \AA}$ ,  $b = 17.828(4) \text{ \AA}$ ,  $c = 4.585(1) \text{ \AA}$ ,  $V = 678.4(2) \text{ \AA}^3$ ,  $Z = 4$ ,  $M = 605.4(1)$ ,  $D_{\text{calc}} = 2.37(1) \text{ g cm}^{-3}$ , Mo  $K\alpha$ ,  $R_{\text{F}} = 0.03$ . In **I**, the Sn atoms are hexacoordinated with oxygen and form porous tin oxalate sheets with the protonated diamine sitting in the middle of the pore, while, in **II**, four-coordinated Sn atoms form tin oxalate monomer units which are held together by the protonated guanidium cations. In **III**, we again see the presence of the anionic tin oxalate monomer units hydrogen bonded to the protonated 1,5-diaminopentane cations giving rise to one-dimensional ribbons. These amine-containing oxalate materials constitute a new family of structures where hydrogen bonding interactions, involving the amines, play an important role. The observation of six-coordination for tin in **I** which forms a pseudo pentagonal bipyramid akin to that in a 14 electron system is noteworthy. The novel features of oxalate **I–III** suggest that exploration of various metal dicarboxylates prepared in the presence of structure-directing agents may indeed yield new types of interesting structures with unusual coordination.

## Introduction

Nanoporous inorganic materials, such as the aluminosilicate zeolites, aluminum phosphates, and a host of related materials, have been extensively studied during recent years and are of great interest on account of their utility, both potential and actual, as molecular sieves, catalysts, and ion-exchange media.<sup>1</sup> During the past decade, there has also been a parallel development in the synthesis of open-framework coordination compounds by self-assembly. The object of self-assembly is to put together a set of molecules, with matching functional groups along with structure-directing agents, so that they join together in a predefined manner. These materials, in a sense, can be classified as framework solids that we design rather than the materials waiting to be discovered. Rational design of such materials, however, remains primitive, because of the interplay of

several factors such as ligand–donor group geometry, stereochemistry, solvent, coordination preferences and oxidation states of the metal ions, and the nature of the counterion. One of the approaches for formulating a mechanism for the formation of such tailored solids would be to synthesize many structures in as many systems with several topologies so as to develop the skill and possibly thumb rules to define the structure–property–function relations.

In the late 1980's and 1990's, there has been considerable research interest in producing new and novel frameworks, different from the traditional tetrahedra-linked materials (zeolites, AlPO's, etc.). The choice of frameworks has widened considerably, with chalcogenides, pnictides, cyanides, thiopnictates, and some rigid bidentate ligands being linked with metal centers to form new classes of open-framework materials. New developments in the area of framework solids have been reviewed recently.<sup>2</sup> Some of the recent examples of framework materials include transition metal diphos-

\* Corresponding author.

<sup>†</sup> University of California.

<sup>‡</sup> Jawaharlal Nehru Centre for Advanced Scientific Research.

(1) Thomas, J. M. *Angew. Chem., Intl. Ed. Engl.* **1994**, *33*, 913.

(2) Bowes, C. L.; Ozin, G. A. *Adv. Mater.* **1996**, *8*, 13.

**Table 1. Crystal Data and Structure Refinement Parameters of I, [(CH<sub>3</sub>)<sub>2</sub>NH(CH<sub>2</sub>)<sub>4</sub>NH(CH<sub>3</sub>)<sub>2</sub>]<sup>2+</sup>[Sn<sub>2</sub>(C<sub>2</sub>O<sub>4</sub>)<sub>3</sub>]<sup>2-</sup>, II, [C(NH<sub>2</sub>)<sub>3</sub>]<sub>2</sub><sup>+</sup>[Sn<sub>2</sub>(C<sub>2</sub>O<sub>4</sub>)<sub>3</sub>]<sup>2-</sup>·2H<sub>2</sub>O, and III, [C<sub>5</sub>N<sub>2</sub>H<sub>16</sub>]<sup>2+</sup>[Sn<sub>2</sub>(C<sub>2</sub>O<sub>4</sub>)<sub>3</sub>]<sup>2-</sup>**

	compd I	compd II	compd III
empirical formula	Sn <sub>2</sub> O <sub>12</sub> N <sub>2</sub> C <sub>14</sub> H <sub>22</sub>	Sn <sub>2</sub> O <sub>14</sub> N <sub>6</sub> C <sub>8</sub> H <sub>16</sub>	Sn <sub>2</sub> O <sub>12</sub> N <sub>2</sub> C <sub>11</sub> H <sub>16</sub>
cryst syst	monoclinic	triclinic	orthorhombic
space group	<i>P</i> 2 <sub>1</sub> / <i>c</i> (No. 14)	<i>P</i> 1̄ (no. 2)	<i>P</i> mmn (No. 59)
cryst size (mm)	0.04 × 0.1 × 0.06	0.06 × 0.06 × 0.12	0.16 × 0.14 × 0.04
<i>a</i> (Å)	8.427(2)	7.564(1)	8.281(2)
<i>b</i> (Å)	14.257(1)	10.633(1)	17.828(4)
<i>c</i> (Å)	8.868(2)	12.050(1)	4.595(1)
α (deg)	90.0	87.9(1)	90.0
β (deg)	100.3(1)	85.2(1)	90.0
γ (deg)	90.0	85.9(1)	90.0
vol (Å <sup>3</sup> )	1048.3(2)	962.8(1)	678.4(2)
<i>Z</i>	4	2	2
formula mass	647.4(1)	657.5(1)	605.4(1)
ρ <sub>calc</sub> (g cm <sup>-3</sup> )	2.06(1)	2.25(1)	2.37(1)
λ (Mo Kα) (Å)	0.710 73	0.710 73	0.710 73
μ (mm <sup>-1</sup> )	2.45	2.68	3.72
2θ range (deg)	5.0–50.0	3–50.0	4.5–47
total data collectd	5080	8291	2348
index ranges	–11 ≤ <i>h</i> ≤ +10, 0 ≤ <i>k</i> ≤ +18, 0 ≤ <i>l</i> ≤ +11	–9 ≤ <i>h</i> ≤ +10, –13 ≤ <i>k</i> ≤ +14, 0 ≤ <i>l</i> ≤ +15	–8 ≤ <i>h</i> ≤ +9, –18 ≤ <i>k</i> ≤ +19, –4 ≤ <i>l</i> ≤ +5
unique data	2362	4309	2348
obsd data (σ > 3σ( <i>I</i> ))	1463	2811	544
refinement method	full-matrix least-squares on   <i>F</i>	full-matrix least-squares on   <i>F</i>	full-matrix least-squares on   <i>F</i> <sup>2</sup>
<i>R</i> <sub>merg</sub>	10.8	11.7	4.0
<i>R</i> indexes [ <i>I</i> > 3σ( <i>I</i> )]	<i>R</i> <sub>F</sub> = 5.51%; <i>R</i> <sub>w<i>F</i><sup>2</sup></sub> = 6.07%	<i>R</i> <sub>F</sub> = 6.30%; <i>R</i> <sub>w<i>F</i><sup>2</sup></sub> = 6.76%	<i>R</i> <sub>F</sub> = 3.28%; <i>R</i> <sub>w<i>F</i><sup>2</sup></sub> = 6.5%
goodness of fit ( <i>S</i> )	1.06	1.08	1.16
no. of variables	147	282	72
largest diff map peak and hole (e Å <sup>-3</sup> )	+0.77 and –0.77	+1.13 and –1.81	+0.29 and –0.53

phonates,<sup>3–5</sup> complexes of bridging amines such as 2,2'-bipyridine,<sup>6,7</sup> 4,4'-bipyridine,<sup>8–11</sup> and 2,2'-bipyridine,<sup>12,13</sup> and dicarboxylate complexes of rare earths and transition metals.<sup>14–16</sup> While organic cations, such as quaternary amines, play a crucial role in the formation of inorganic sieve structures, where they act as template molecules or structure-directing agents,<sup>17</sup> recent studies have shown that, in the area of open-framework coordination compounds, a variety of traditional and non-traditional structure-directing agents can be used to yield new carboxylates and other related materials.<sup>18–20</sup>

As part of a program to produce new varieties of open-framework materials, we have been exploring compounds formed by metal dicarboxylates in the presence of traditional structure-directing agents, such as organic amines. In the present work, we describe the synthesis of three members of a new family of tin(II) oxalates, incorporating the amines, with novel structural features. The results suggest the likely occurrence of a whole variety of new materials, some of which would have open-framework structure, formed in the presence of organic amines by different combinations of dicarboxylic acids and metal ions.

## Experimental Section

**Synthesis and Initial Characterization.** Tin(II) oxalate open-framework structures, **I–III**, were synthesized starting from a mixture containing *N,N,N,N*-tetramethyl-1,4-diaminobutane (TMDAB) (**I**), guanidium carbonate (GC) (**II**), or 1,5-diaminopentane (**III**), respectively, as the structure-directing agent. For **I**, tin(II) oxalate (Aldrich), phosphoric acid (85 wt %, Aldrich), TMDAB, water, and ethylene glycol (EG) in the ratio 1:0.5:1:33:6 SnC<sub>2</sub>O<sub>4</sub>:P<sub>2</sub>O<sub>5</sub>:TMDAB:H<sub>2</sub>O:EG were taken in the starting mixture (EG was added to control the pressure within the bomb). For **II**, tin oxalate, phosphoric acid, GC, and water were mixed in the ratio 1.0:0.75:1.0:SnC<sub>2</sub>O<sub>4</sub>:P<sub>2</sub>O<sub>5</sub>:GC:H<sub>2</sub>O. For **III**, tin oxalate, phosphoric acid, amine, and water were mixed in the ratio 1.0:0.5:1.0:55 SnC<sub>2</sub>O<sub>4</sub>:P<sub>2</sub>O<sub>5</sub>:amine:H<sub>2</sub>O. The starting mixtures were stirred to attain homogeneity and then sealed in PTFE-lined stainless steel autoclaves (Parr). The sealed pressure bombs were heated at 140 °C for 2 days under autogeneous pressure. In the case of **III**, the bombs were maintained at 180 °C for a further period of 2 days. The resulting products, predominantly contained large quantities of single crystals. The crystals were filtered and washed thoroughly with deionized water. Powder X-ray diffraction

- (3) Johnson, J. W.; Jacobson, A. J.; Butler, W. M.; Rosenthal, S. E.; Brody, J. F.; Lewandowski, J. T. *J. Am. Chem. Soc.* **1989**, *111*, 381.  
 (4) LaDuca, R.; Rose, D.; Debord, J. R. D.; Haushalter, R. C.; O'Connor, C. J.; Zubieta, J. *J. Solid State Chem.* **1996**, *123*, 408.  
 (5) Drumel, S.; Janvier, P.; Barbois, P.; Bujoli-Doeuff, M.; Bujoli, B. *Inorg. Chem.* **1995**, *34*, 148, and references cited therein.  
 (6) Zhang, Y.; DeBord, J. R. D.; O'Connor, C. J.; Haushalter, R.; Clearfield, A.; Zubieta, J. *Angew. Chem., Int. Ed. Engl.* **1996**, *35*, 989.  
 (7) Zapf, P. J.; Hammond, R. P.; Haushalter, R. C.; Zubieta, J. *Chem. Mater.* **1998**, *10*, 1366.  
 (8) Losier, P.; Zaworotko, M. J. *Angew. Chem., Int. Ed. Engl.* **1996**, *35*, 2779. Zaworotko, M. J. *Chem. Soc. Rev.* **1994**, 283.  
 (9) Yaghi, O. M.; Li, H. *Angew. Chem., Int. Ed. Engl.* **1995**, *34*, 207.  
 Yaghi, O. M.; Li, H. *J. Am. Chem. Soc.* **1997**, *119*, 10867.  
 (10) Yaghi, O. M.; Li, H. *Nature* **1995**, *378*, 703.  
 (11) Pedireddi, V. R.; Chatterjee, S.; Ranganathan, A.; Rao, C. N. R. *J. Am. Chem. Soc.* **1997**, *119*, 10867.  
 (12) De Munno, G.; Ruiz, R.; Lloret, F.; Faus, J.; Sessoli, R.; Julve, M. *Inorg. Chem.* **1995**, *34*, 408, and references cited therein.  
 (13) Decurtins, S.; Schmalle, H. W.; Schneuwly, P.; Zhang, L.-M.; Enslin, J.; Hauser, A. *Inorg. Chem.* **1995**, *34*, 5501, and references cited therein.  
 (14) Serpaggi, F.; Férey, G. *J. Mater. Chem.*, in press.  
 (15) Livage, C.; Egger, C.; Nogues, C.; Férey, G. *J. Mater. Chem.*, in press.  
 (16) Romero, S.; Mosset, A.; Trombe, J. C. *Euro. J. Solid State Inorg. Chem.* **1997**, *34*, 209.  
 (17) Davis, M. E.; Lobo, R. F. *Chem. Mater.* **1992**, *4*, 756.  
 (18) Clemente-Leon, M.; Coronado, E.; Galan-Mascaros, J.-R.; Comez-García, C. *J. Chem. Commun.* **1997**, 1727.  
 (19) Farrell, S. P.; Hambley, T. W.; Lay, P. A. *Inorg. Chem.* **1995**, *34*, 757.  
 (20) Kitagawa, S.; Okubo, T.; Kawata, S.; Kondo, M.; Katada, M.; Kobayashi, H. *Inorg. Chem.* **1995**, *34*, 4790.

**Table 2. Atomic Coordinates and Isotropic Thermal Parameters for the Non-Hydrogen Atoms in I, [(CH<sub>3</sub>)<sub>2</sub>NH(CH<sub>2</sub>)<sub>4</sub>NH(CH<sub>3</sub>)<sub>2</sub>]<sup>2+</sup>[Sn<sub>2</sub>(C<sub>2</sub>O<sub>4</sub>)<sub>3</sub>]<sup>2-</sup>**

atom	x	y	z	U <sub>eq</sub> /U <sub>iso</sub>
Sn(1)	0.19440(9)	0.40047(4)	0.09075(6)	0.0418
O(1)	0.3191(7)	0.2804(5)	0.0223(6)	0.0420
O(2)	0.515(2)	0.5514(7)	-0.1739(8)	0.0645
O(3)	0.3270(8)	0.1696(4)	-0.1510(6)	0.0431
O(4)	0.0386(8)	0.3429(5)	-0.1338(7)	0.0511
O(5)	0.0428(8)	0.2327(7)	-0.3119(7)	0.0533
O(6)	0.315(2)	0.4693(9)	-0.1082(9)	0.0853
C(10)	0.2623(9)	0.2376(5)	-0.1026(7)	0.0265
C(20)	0.100(1)	0.2737(7)	-0.1922(8)	0.0341
C(30)	0.451(3)	0.504(1)	-0.082(1)	0.0674
C(1)	0.075(1)	0.9755(8)	-0.015(1)	0.0587
C(2) <sup>a</sup>	0.215(3)	0.975(2)	0.085(2)	0.0578
C(2A) <sup>a</sup>	0.118(3)	0.888(1)	0.052(2)	0.0426
N(1)	0.314(2)	0.876(1)	0.058(1)	0.0710
C(3)	0.366(2)	0.892(1)	-0.097(1)	0.0759
C(4)	0.294(2)	0.780(2)	0.087(2)	0.0982

<sup>a</sup> Occupancy 0.51 and 0.49, respectively.**Table 3. Selected Interatomic Distances in I, [(CH<sub>3</sub>)<sub>2</sub>NH(CH<sub>2</sub>)<sub>4</sub>NH(CH<sub>3</sub>)<sub>2</sub>]<sup>2+</sup>[Sn<sub>2</sub>(C<sub>2</sub>O<sub>4</sub>)<sub>3</sub>]<sup>2-</sup>**

moiety	distance (Å)	moiety	distance (Å)
Framework			
Sn(1)–O(1)	2.152(6)	Sn(1)–O(2)	2.52(1)
Sn(1)–O(3)	2.565(6)	Sn(1)–O(4)	2.330(7)
Sn(1)–O(5)	2.525(8)	Sn(1)–O(6)	2.397(8)
O(1)–C(10)	1.281(8)	O(2)–C(30)	1.25(1)
O(3)–C(10)	1.227(9)	O(4)–C(20)	1.27(1)
O(5)–C(20)	1.23(1)	O(6)–C(30)	1.23(2)
C(10)–C(20)	1.54(1)	C(30)–C(30)	1.54(3)
Organic Moiety			
C(1)–C(1)	1.52(2)	C(1)–C(2)	1.34(2)
C(1)–C(2A)	1.40(2)	C(2)–N(1)	1.685(1)
C(2A)–N(1)	1.649(1)	N(1)–C(3)	1.53(2)
N(1)–C(4)	1.41(3)		

**Table 4. Selected Bond Angles in I, [(CH<sub>3</sub>)<sub>2</sub>NH(CH<sub>2</sub>)<sub>4</sub>NH(CH<sub>3</sub>)<sub>2</sub>]<sup>2+</sup>[Sn<sub>2</sub>(C<sub>2</sub>O<sub>4</sub>)<sub>3</sub>]<sup>2-</sup>**

moiety	angle (deg)	moiety	angle (deg)
Framework			
O(1)–Sn(1)–O(2)	78.5(3)	O(1)–Sn(1)–O(3)	77.6(2)
O(2)–Sn(1)–O(3)	66.4(2)	O(1)–Sn(1)–O(4)	73.0(2)
O(2)–Sn(1)–O(4)	135.6(2)	O(3)–Sn(1)–O(4)	135.7(2)
O(1)–Sn(1)–O(5)	78.5(3)	O(2)–Sn(1)–O(5)	128.9(3)
O(3)–Sn(1)–O(5)	64.4(2)	O(4)–Sn(1)–O(5)	77.6(2)
O(1)–Sn(1)–O(6)	80.0(4)	O(2)–Sn(1)–O(6)	65.7(4)
O(3)–Sn(1)–O(6)	130.0(4)	O(4)–Sn(1)–O(6)	76.3(3)
O(5)–Sn(1)–O(6)	150.0(3)	O(1)–C(10)–O(3)	123.9(7)
O(4)–C(20)–O(5)	126.4(8)	O(2)–C(30)–O(6)	126.0(2)
Organic Moiety			
C(1)–C(1)–C(2)	123.1(2)	C(1)–C(1)–C(2A)	119.6(2)
C(1)–C(2)–N(1)	108.0(2)	C(1)–C(2A)–N(1)	106.8(3)
C(3)–N(1)–C(4)	112.0(2)	C(4)–N(1)–C(2)	135.3(3)
C(4)–N(1)–C(2A)	113.5(1)	C(2)–N(1)–C(3)	103.1(3)
C(4)–N(1)–C(2A)	87.5(1)		

(XRD) patterns on the powdered crystals indicated that the products were new materials. Thermogravimetric analysis (TGA) was carried out in static air in the range from 25 to 900 °C.

**Single-Crystal Structure Determination.** A suitable single crystal of each compound was carefully selected under a polarizing microscope and glued to a thin glass fiber with cyanoacrylate (superglue) adhesive. Crystal structure determination by X-ray diffraction was performed on a Siemens Smart-CCD diffractometer equipped with a normal focus, 2.4 kW sealed tube X-ray source (Mo K $\alpha$  radiation,  $\lambda = 0.71073$  Å) operating at 50 kV and 40 mA. A hemisphere of intensity data were collected at room temperature in 1321 frames with  $\omega$  scans (width of 0.30° and exposure time of 20 s per frame). The final unit cell constants were determined by a least

**Table 5. Atomic Coordinates and Isotropic Thermal Parameters for the Non-Hydrogen Atoms in II, [(NH<sub>2</sub>)<sub>3</sub>]<sup>+</sup>[Sn<sub>2</sub>(C<sub>2</sub>O<sub>4</sub>)<sub>3</sub>]<sup>2-</sup>·2H<sub>2</sub>O**

atom	x	y	z	U <sub>eq</sub> /U <sub>iso</sub>
Sn(1)	0.18340(9)	0.33924(6)	0.02038(6)	0.0257
Sn(2)	0.6355(1)	0.14758(6)	0.17654(6)	0.0331
O(1)	0.0835(9)	0.5104(6)	0.1132(6)	0.0279
O(2)	0.4373(9)	0.3755(6)	0.0918(6)	0.0275
O(3)	0.082(1)	0.2753(6)	0.1924(6)	0.0287
O(4)	0.323(1)	0.5163(7)	-0.0844(6)	0.0339
O(5)	0.446(1)	0.2250(6)	0.3102(6)	0.0346
O(6)	0.4003(9)	0.1221(6)	0.0837(6)	0.0299
O(7)	0.541(1)	-0.0150(6)	0.2775(7)	0.0347
O(8)	0.703(1)	-0.0297(8)	0.0546(7)	0.0411
O(9)	-0.089(1)	0.3341(8)	0.3417(7)	0.0467
O(10)	-0.062(1)	0.5798(7)	0.2684(6)	0.0365
O(11)	0.265(1)	0.1784(8)	0.4588(7)	0.0442
O(12)	0.361(1)	-0.0737(7)	0.4246(7)	0.0394
O(100) <sup>a</sup>	0.583(1)	0.7252(8)	0.2415(8)	0.0448
O(200) <sup>a</sup>	0.257(2)	0.758(1)	0.126(1)	0.0657
C(1)	0.004(1)	0.4962(9)	0.2088(9)	0.0272
C(2)	0.535(1)	0.4594(8)	0.0511(7)	0.0211
C(3)	-0.005(1)	0.355(1)	0.2531(9)	0.0320
C(4)	0.375(1)	0.145(1)	0.3808(9)	0.0325
C(5)	0.414(1)	0.0436(9)	0.0081(9)	0.0309
C(6)	0.429(1)	0.005(1)	0.3608(9)	0.0340
C(10)	0.319(2)	0.536(1)	0.4292(9)	0.0346
C(20)	-0.023(2)	-0.034(1)	0.3157(9)	0.0299
N(11)	0.233(1)	0.4513(9)	0.4950(8)	0.0381
N(12)	0.404(1)	0.4977(9)	0.3349(8)	0.0385
N(13)	0.314(2)	0.6545(9)	0.4560(9)	0.0408
N(21)	-0.097(1)	0.0555(9)	0.3807(9)	0.0403
N(22)	-0.047(1)	-0.1520(8)	0.3391(9)	0.0351
N(23)	0.081(1)	-0.001(1)	0.2238(8)	0.0416

<sup>a</sup> Water molecules.**Table 6. Selected Interatomic Distances in II, [(NH<sub>2</sub>)<sub>3</sub>]<sup>+</sup>[Sn<sub>2</sub>(C<sub>2</sub>O<sub>4</sub>)<sub>3</sub>]<sup>2-</sup>·2H<sub>2</sub>O**

moiety	distance (Å)	moiety	distance (Å)
Framework			
Sn(1)–O(1)	2.224(7)	Sn(1)–O(2)	2.233(7)
Sn(1)–O(3)	2.248(7)	Sn(1)–O(4)	2.477(7)
Sn(2)–O(5)	2.207(8)	Sn(2)–O(6)	2.218(7)
Sn(2)–O(7)	2.203(7)	Sn(2)–O(8)	2.431(8)
C(1)–O(1)	1.26(1)	C(2)–O(2)	1.26(1)
C(1)–O(10)	1.22(1)	C(2)–O(4)	1.22(1)
C(3)–O(3)	1.25(1)	C(4)–O(5)	1.29(1)
C(3)–O(9)	1.22(1)	C(4)–O(11)	1.25(1)
C(5)–O(6)	1.25(1)	C(6)–O(7)	1.27(1)
C(5)–O(8)	1.23(1)	C(6)–O(12)	1.23(1)
C(1)–C(3)	1.58(1)	C(2)–C(2)	1.59(2)
C(4)–C(6)	1.53(1)	C(5)–C(5)	1.55(2)
Organic moiety			
C(10)–N(11)	1.34(1)	C(20)–N(21)	1.32(2)
C(10)–N(12)	1.32(1)	C(20)–N(22)	1.30(1)
C(10)–N(13)	1.31(1)	C(20)–N(23)	1.35(1)

squares fit of 2762 reflections for **I**, 5873 reflections for compound **II**, and 1586 reflections for compound **III** in the range  $3^\circ < 2\theta < 46.5^\circ$ . Pertinent experimental details for the structure determinations are presented in Table 1.

The structure was solved by direct methods using SHELXS-86<sup>21</sup> and difference Fourier syntheses. All of the hydrogen positions were initially located in the difference Fourier map for compounds **I–III**. For the final refinement of **I** and **III**, the hydrogen atoms were placed geometrically, and for **II**, the hydrogen atoms of the amine molecules were placed assuming a planar sp<sup>2</sup> hybridization about each N atom and an N–H bond length of 0.95 Å, and held in the riding mode for all the compounds. An empirical absorption correction based on the DIFABS calculation routine was applied for compounds **I** and **II** (DIFABS minimum and maximum correction: 0.90 and 1.14

(21) Sheldrick, G. M. *SHELXL-86, A program for the solution of crystal structures*; University of Göttingen: Göttingen, Germany, 1993.

**Table 7. Selected Bond Angles in II,**  
[C(NH<sub>2</sub>)<sub>3</sub>]<sub>2</sub><sup>+</sup>[Sn<sub>2</sub>(C<sub>2</sub>O<sub>4</sub>)<sub>3</sub>]<sup>2-</sup>·2H<sub>2</sub>O

moiety	angle (deg)	moiety	angle (deg)
Framework			
O(1)–Sn(1)–O(2)	82.6(3)	O(1)–Sn(1)–O(3)	72.5(2)
O(2)–Sn(1)–O(3)	87.5(3)	O(1)–Sn(1)–O(4)	75.0(3)
O(2)–Sn(1)–O(4)	70.3(2)	O(3)–Sn(1)–O(4)	142.5(3)
O(5)–Sn(2)–O(7)	73.4(3)	O(5)–Sn(2)–O(6)	86.5(3)
O(7)–Sn(2)–O(6)	83.5(3)	O(5)–Sn(2)–O(8)	143.9(3)
O(7)–Sn(2)–O(8)	76.1(3)	O(6)–Sn(2)–O(8)	71.2(2)
O(1)–C(1)–O(10)	126.3(9)	O(2)–C(2)–O(4)	125.7(8)
O(3)–C(3)–O(9)	126.5(10)	O(5)–C(4)–O(11)	121.9(10)
O(6)–C(5)–O(8)	123.9(10)	O(7)–C(6)–O(12)	127.4(10)
O(1)–C(1)–C(3)	115.2(8)	O(2)–C(2)–C(2)	116.0(10)
O(3)–C(3)–C(1)	114.8(8)	O(4)–C(2)–C(2)	118.3(10)
O(5)–C(4)–C(6)	116.2(9)	O(6)–C(5)–C(5)	119.1(11)
O(7)–C(6)–C(4)	114.7(9)	O(8)–C(5)–C(5)	117.0(11)
O(9)–C(3)–C(1)	118.7(9)	O(10)–C(1)–C(3)	118.4(9)
O(11)–C(4)–C(6)	121.9(10)	O(12)–C(6)–C(4)	117.9(10)
Organic moiety			
N(11)–C(10)–N(12)	118.4(10)	N(21)–C(20)–N(22)	121.1(11)
N(11)–C(10)–N(13)	120.8(10)	N(21)–C(20)–N(23)	118.8(10)
N(12)–C(10)–N(13)	120.8(10)	N(22)–C(20)–N(23)	119.9(11)

**Table 8. Atomic Coordinates and Isotropic Thermal Parameters for the Non-Hydrogen Atoms in III,**  
[C<sub>5</sub>N<sub>2</sub>H<sub>16</sub>]<sup>2+</sup>[Sn<sub>2</sub>(C<sub>2</sub>O<sub>4</sub>)<sub>3</sub>]<sup>2-</sup>

atom	x	y	z	U <sub>eq</sub> /U <sub>iso</sub>
Sn(1)	0.2500	0.7500	0.7268(1)	0.033
O(1)	0.0917(4)	0.6717(2)	0.9672(7)	0.042
O(2)	0.0853(4)	0.5649(2)	1.2186(7)	0.051
C(10)	0.1578(5)	0.6164(2)	1.0972(9)	0.033
N(1)	0.2500	0.4574(3)	0.5999(1)	0.034
C(1)	0.2500	0.3919(3)	0.4013(1)	0.035
C(2)	0.2500	0.3201(3)	0.5754(1)	0.031
C(3)	0.2500	0.2500	0.3898(2)	0.033

for **I** and 0.92 and 1.08 for **II**). No absorption correction was applied for compound **III**. The last cycles of refinement included atomic positions for all of the atoms, anisotropic thermal parameters for all non-hydrogen atoms, and isotropic thermal parameters for all of the hydrogen atoms. The applied weighting scheme was that of Tukey and Prince based on a three-term modified Chebyshev polynomial<sup>22</sup> for compounds **I** and **II**. Full-matrix least-squares structure refinement against  $|F|$  for compounds **I** and **II** was carried out using the CRYSTALS<sup>23</sup> package of programs and by SHELXTL-PLUS<sup>24</sup> for compound **III**. Details of the final refinements are given in Table 1. The final atomic coordinates, selected bond distances, and bond angles are given for **I** in Tables 2–4, for **II** in Tables 5–7, and for **III** in Tables 8 and 9.

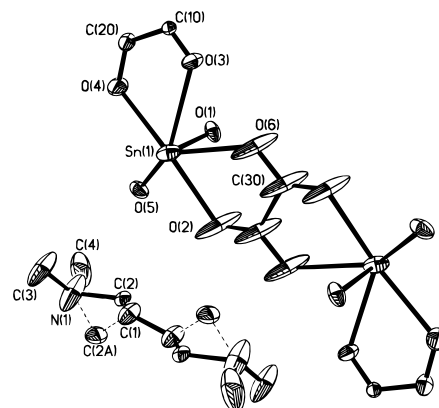
## Results

**Structure of I,** [(CH<sub>3</sub>)<sub>2</sub>NH(CH<sub>2</sub>)<sub>4</sub>NH(CH<sub>3</sub>)<sub>2</sub>]<sup>2+</sup>·[Sn<sub>2</sub>(C<sub>2</sub>O<sub>4</sub>)<sub>3</sub>]<sup>2-</sup>. The asymmetric unit of **I** contains 15 non-hydrogen atoms (Figure 1a), and the structure consists of macroanionic sheets of formula [Sn(C<sub>2</sub>O<sub>4</sub>)<sub>1.5</sub>]<sup>-</sup> with interlamellar [(CH<sub>3</sub>)<sub>2</sub>NH(CH<sub>2</sub>)<sub>4</sub>NH(CH<sub>3</sub>)<sub>2</sub>]<sup>2+</sup> ions. The individual layers consist of a network of SnO<sub>6</sub> and C<sub>2</sub>O<sub>4</sub> moieties with each Sn atom bound to six oxygens, which are, in turn, bound to carbon atoms forming the network structure. Conversely, the oxalate ions are

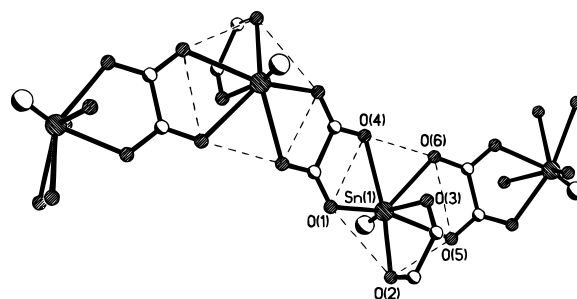
**Table 9. Selected Bond Distances and Angles in III,**  
[C<sub>5</sub>N<sub>2</sub>H<sub>16</sub>]<sup>2+</sup>[Sn<sub>2</sub>(C<sub>2</sub>O<sub>4</sub>)<sub>3</sub>]<sup>2-</sup>

moiety	distance (Å)	moiety	angle (deg)
Sn(1)–O(1)	2.11(3)	O(1)–Sn(1)–O(1) <sup>a</sup>	78.3(2)
Sn(1)–O(1) <sup>a</sup>	2.113(3)	O(1)–Sn(1)–O(1) <sup>b</sup>	120.0(2)
Sn(1)–O(1) <sup>b</sup>	2.113(3)	O(1) <sup>a</sup> –Sn(1)–O(1) <sup>b</sup>	72.8(2)
Sn(1)–O(1) <sup>c</sup>	2.113(3)	O(1)–Sn(1)–O(1) <sup>c</sup>	72.8(2)
C(10)–O(1)	1.276(5)	O(1) <sup>a</sup> –Sn(1)–O(1) <sup>c</sup>	120.0(2)
C(10)–O(2)	1.232(5)	O(1) <sup>b</sup> –Sn(1)–O(1) <sup>c</sup>	78.3(2)
C(10)–C(10) <sup>c</sup>	1.526(9)	O(1)–C(10)–O(2)	125.4(4)
Organic Moiety			
N(1)–C(1)	1.483(8)	N(1)–C(1)–C(2)	110.0(5)
C(1)–C(2)	1.508(9)	C(1)–C(2)–C(3)	113.7(5)
C(2)–C(3)	1.513(7)	C(2)–C(3)–C(2) <sup>d</sup>	111.4(7)
C(3)–C(2) <sup>d</sup>	1.513(7)		

<sup>a</sup> Structure coordinates:  $x, -y + 3/2, z$ . <sup>b</sup> Structure coordinates:  $-x + 1/2, -y + 3/2, z$ . <sup>c</sup> Structure coordinates:  $-x + 1/2, y, z$ . <sup>d</sup> Structure coordinates:  $-x + 1/2, -y + 1/2, z$ .



(a)



(b)

**Figure 1.** (a) ORTEP plot of **I**, [(CH<sub>3</sub>)<sub>2</sub>NH(CH<sub>2</sub>)<sub>4</sub>NH(CH<sub>3</sub>)<sub>2</sub>]<sup>2+</sup>·[Sn<sub>2</sub>(C<sub>2</sub>O<sub>4</sub>)<sub>3</sub>]<sup>2-</sup>, showing the connectivity (the asymmetric unit is labeled). Hydrogens on the amines are not shown. The dotted line represents the disorder in the amine. Thermal ellipsoids are given at 30% probability. (b) Coordination environment (pentagonal bipyramid) around the central Sn atom (partly filled circles represent the lone pair of electrons). As can be seen, the lone pair of the neighboring Sn atoms points in the opposite direction.

connected to the tin atoms forming the architecture. In the SnO<sub>6</sub> units, five oxygens lie in a plane forming a pentagon, with the sixth oxygen along with the lone pair of electrons forming two vertices, above and below the plane of the pentagon (Figure 1b). To our knowledge, this is the first time such a building unit has been observed for an open-framework material. This resembles the classic 14 electron species observed in interhalogen compounds such as [IF<sub>6</sub>]<sup>-</sup>. These pentagonal bipyramidal units (Figure 1b) are arranged in such

(22) (a) Prince, E. *Mathematical Techniques in Crystallography and Materials Science*; Springer-Verlag: New York, 1982; p 72. (b) Carruthers, J. R.; Watkin, D. J. *Acta Crystallogr.* **1979**, *A35*, 698.

(23) Watkin, D. J.; Carruthers, J. R.; Betteridge, P. W. *CRYSTALS User Guide*; Chemical Crystallography Laboratory, University of Oxford: Oxford, U.K., 1985.

(24) Sheldrick, G. M. *SHELXS-93, Program for Crystal Structure Solution and Refinement*; University of Göttingen: Göttingen, Germany, 1993.

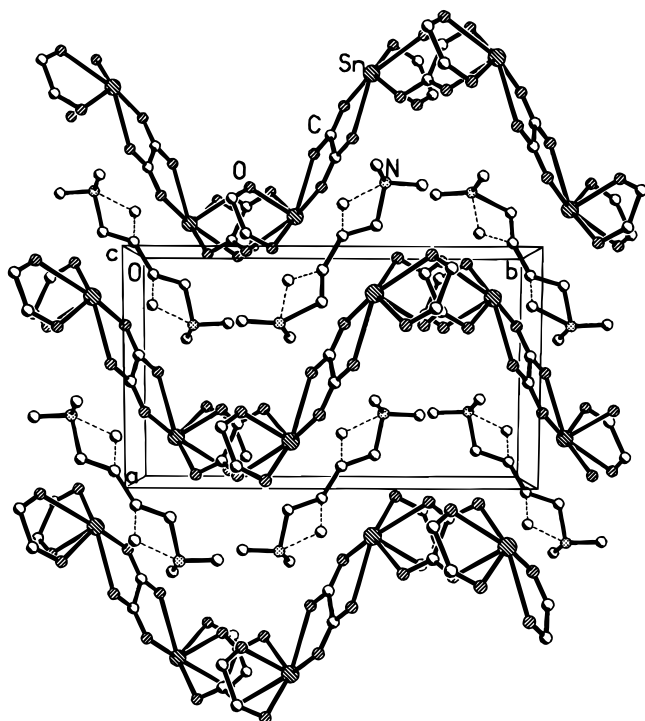


**Figure 2.** Structure of **I**,  $[(\text{CH}_3)_2\text{NH}(\text{CH}_2)_4\text{NH}(\text{CH}_3)_2]^{2+}[\text{Sn}_2(\text{C}_2\text{O}_4)_3]^{2-}$ , viewed along the *c* axis. Alternate layers are formed by the inorganic and organic moieties. The dotted line represents the disorder in the amine. Hydrogens on the amine molecule are not shown for clarity.

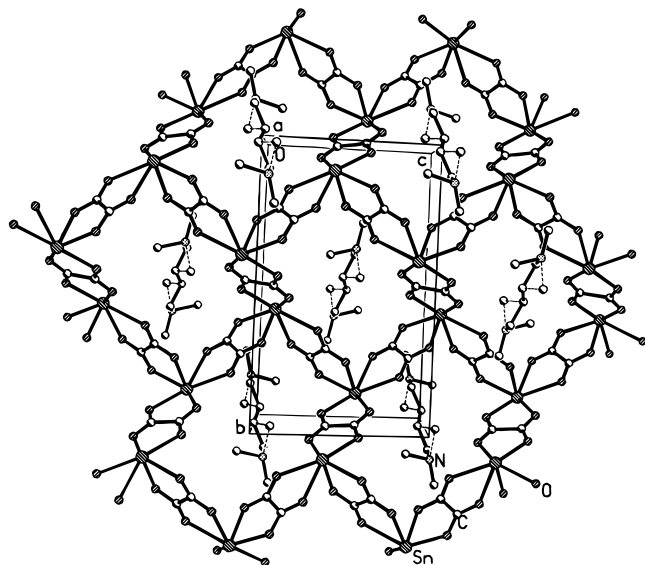
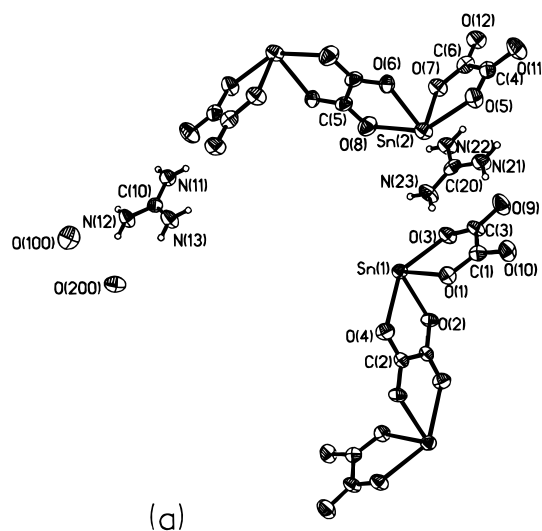
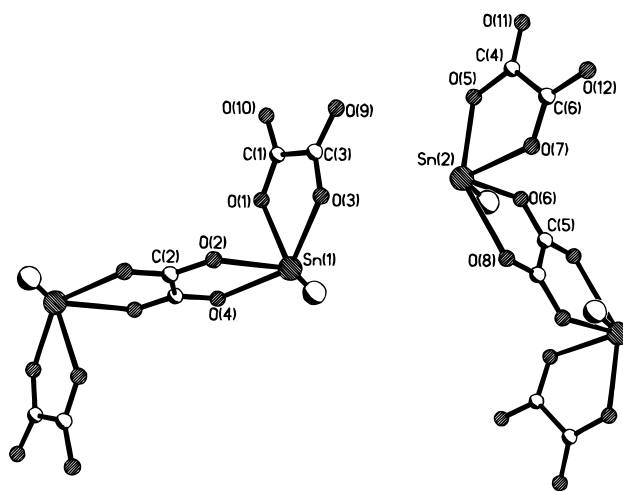


**Figure 3.** Structure of **I**,  $[(\text{CH}_3)_2\text{NH}(\text{CH}_2)_4\text{NH}(\text{CH}_3)_2]^{2+}[\text{Sn}_2(\text{C}_2\text{O}_4)_3]^{2-}$ , viewed along the *a* axis showing the 12-membered ring and the position of the amine molecule. The dotted line represents the disorder in the amine. Hydrogens on the amine molecule are not shown for clarity.

a way that lone pairs of the neighboring Sn atoms point in opposite directions. The structure derives its stability from hydrogen bonded interaction with the protonated diamine which forms alternating puckered layers with the framework, and from the lone pair (projecting into the layers) interactions between the tin(II) atoms (Figure 2). Thus, the structure of **I** provides a basis for evaluating the influence of the Sn(II) lone pair on the structural features and stability of such materials.



(a)



(b)

**Figure 4.** (a) ORTEP plot of **II**,  $[\text{C}(\text{NH}_2)_3]_2^+[\text{Sn}_2(\text{C}_2\text{O}_4)_3]^{2-} \cdot 2\text{H}_2\text{O}$  (the asymmetric unit is labeled). Thermal ellipsoids are given at 50% probability. (b) Arrangement of the lone pair of electrons (partly filled circles represent the lone pair).

A remarkable feature of the structure of **I** is the presence of 12-membered rings within each inorganic sheet (Figure 3). Such perforated sheets have been noticed earlier in a layered AIPO structure.<sup>25</sup> The disposition of the molecules in the interlamellar organic layers is such that, in projection, the protonated *N,N,N,N*-tetramethyl-1,4-diaminobutane is in the middle of the pore formed by the 12-membered rings. The pores penetrate the entire structure in a direction perpendicular to the sheets, thus yielding a solid with unidimensional channels ( $9.486 \times 8.207 \text{ \AA}$ ; longest atom-atom contact distance not including the van der Waals radii) similar to those in aluminosilicate zeolites such as Theta-1<sup>26</sup> and certain detemplated microporous AIPO's (aluminum phosphates).<sup>27</sup> The pores in the inorganic layers of **I** result from the networking between six Sn atoms and six oxalate groups. Of the six oxygens that

(25) Thomas, J. M.; Jones, R. H.; Chen, J.; Xu, R.; Chippindale, A. M.; Natarajan, S.; Cheetham, A. K. *J. Chem. Soc., Chem. Commun.* **1992**, 929.

(26) Barri, S. A. I.; Smith, G. W.; White, E.; Young, D. *Nature* **1985**, *312*, 533.

(27) Wilson, S. T.; Lok, B. M.; Messina, C. A.; Cannon, T. R.; Flannigan, E. M. *J. Am. Chem. Soc.* **1982**, *104*, 1146.

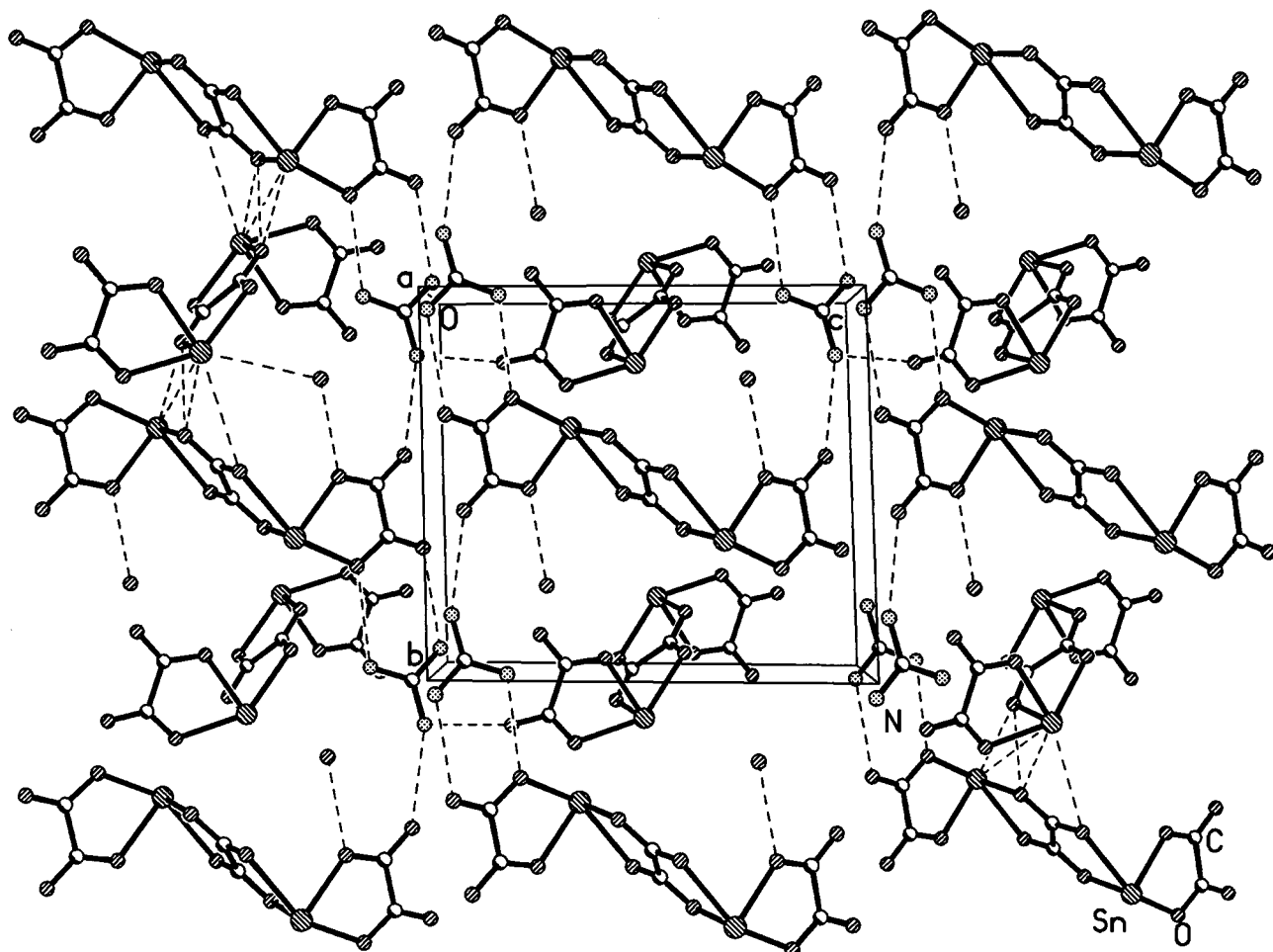


**Figure 5.** Structure of **II**,  $[\text{C}(\text{NH}_2)_3]_2^+[\text{Sn}_2(\text{C}_2\text{O}_4)_3]^{2-} \cdot 2\text{H}_2\text{O}$ , viewed along the  $a$  axis, showing connectivity between the tin oxalate monomers and the amine molecules. Note that the water molecules are situated in the cavities formed by these interactions.

are bound to tin, three are associated with Sn–O distances in the range 2.152–2.397 Å and the other three with distances in the 2.521–2.565 Å range. These are, in most cases, formally the single and double bonded oxygens bound to the carbon atoms, respectively. The variations in the distances are also reflected in the C–O bonding as well (Table 3). The O–Sn–O bond angles are in the range 66.4–150.0° and the O–C–O bond angles in the range 123.9–126.4°. These structural parameters are in the range expected for this type of bonding. Bond valence sum calculations<sup>28</sup> indicated that the valence states of the various species forming the framework are  $\text{Sn}^{2+}$ ,  $\text{C}^{4+}$ ,  $\text{O}^{2-}$ , as expected.

**Structure of II**,  $[\text{C}(\text{NH}_2)_3]_2^+[\text{Sn}_2(\text{C}_2\text{O}_4)_3]^{2-} \cdot 2\text{H}_2\text{O}$ . The asymmetric unit of  $[\text{C}(\text{NH}_2)_3]_2^+[\text{Sn}_2(\text{C}_2\text{O}_4)_3]^{2-} \cdot 2\text{H}_2\text{O}$  is presented in Figure 4a. The structure of this material is built up by hydrogen bonded interactions between inorganic monomers and the organic structure directing agent, viz., the guanidinium cation. The inorganic moiety is composed of Sn atoms bound to four oxygen atoms forming a distorted square pyramidal unit. These  $\text{SnO}_4$  units are, in turn, bound to carbons forming discrete tin oxalate monomer species, which are anionic. There are two different tin oxalate monomer units present in the structure. The lone pair of electrons of the Sn(II) atoms in each of the tin oxalate units are

situated in such a way that they avoid direct interaction (Figure 4b). The individual monomer units consisting of Sn–oxalate–Sn units are puckered with folds occurring at the Sn atoms (Figures 5–7). The inorganic units (tin oxalate monomers) are related to each other via the guanidinium cations through hydrogen bonded interactions (Figures 5–7). The water molecules, present in the material, also participate in hydrogen bonding and are situated in the cavities created by such interactions between the monomer and the amine.

When viewed along the  $a$  axis, the protonated amine and the oxalate monomer species form a zigzag chain type arrangement, creating spaces where the water molecules are present (Figure 5). Along the  $b$  axis, the oxalate anions along with the amine and water molecules form a sheetlike arrangement (Figure 6). Of the two different tin oxalate monomers, one monomer forms a continuous chain along the  $c$  axis, while the other monomer occupies spaces between the chains (Figure 7). The individual chain units are supported by lone pair interactions.

The Sn atoms are four coordinated with respect to the oxygens, forming a truncated square pyramidal unit with Sn–O distances in the range 2.203–2.477 Å (average 2.274 Å). The O–Sn–O bond angles are in the range 70.3–143.9° (average 88.6°). These values are in agreement with the values found for four-coordinated tin(II) atoms. The C–O distances and the C–C distance

(28) Brown, I. D.; Aldermatt, D. *Acta Crystallogr., Sect. B* **1984**, *41*, 244.

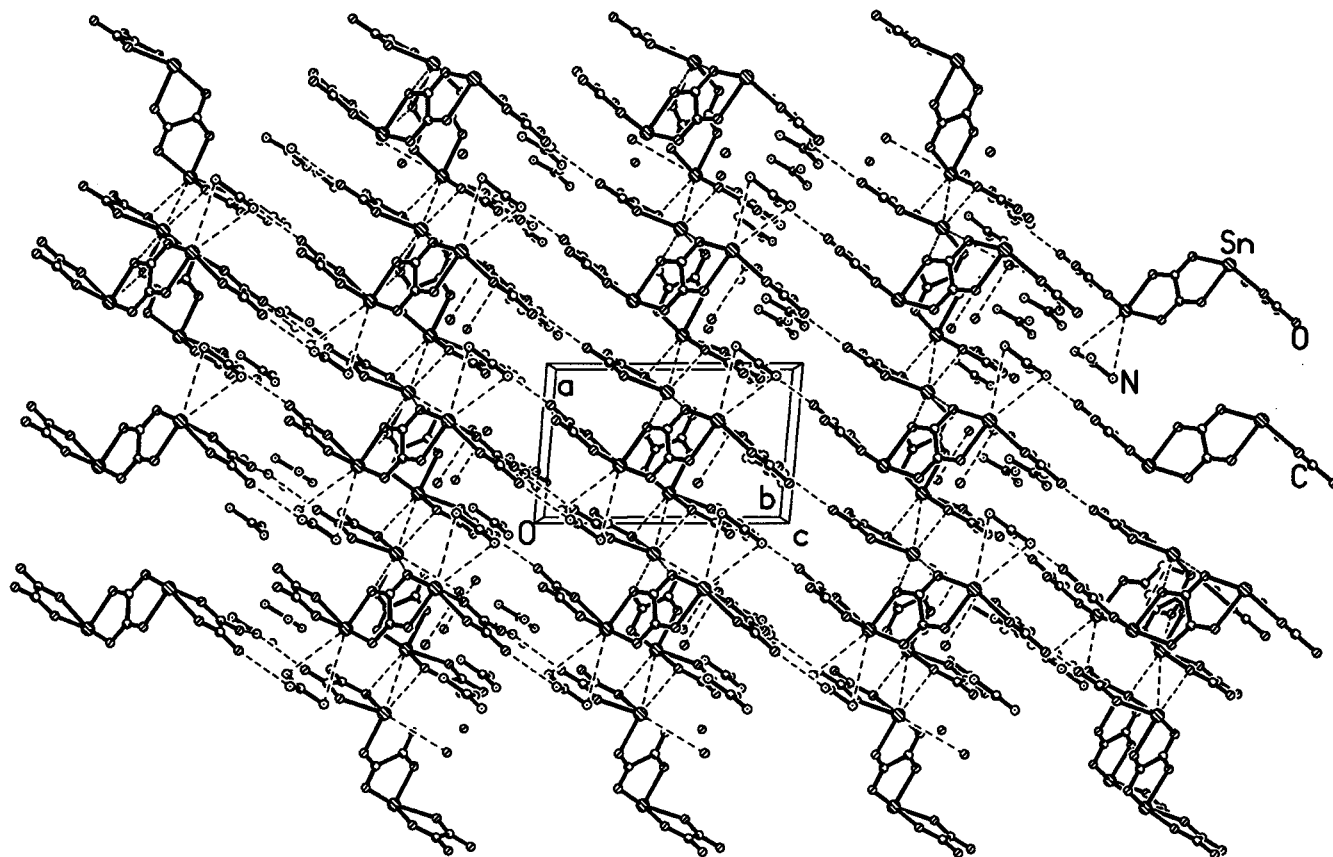


**Figure 6.** Structure of **II**,  $[\text{C}(\text{NH}_2)_3]_2^+[\text{Sn}_2(\text{C}_2\text{O}_4)_3]^{2-} \cdot 2\text{H}_2\text{O}$ , viewed along the  $b$  axis, showing the layer type arrangement created by the hydrogen bonding between the two tin oxalate monomers, the amine and water molecules.

of the oxalate groups are also in agreement with the known values. The complete set of bond distances and bond angles in **II** are presented in Tables 6 and 7.

**Structure of III**,  $[\text{C}_5\text{N}_2\text{H}_{16}]^{2+}[\text{Sn}_2(\text{C}_2\text{O}_4)_3]^{2-}$ . The structure of this material involves hydrogen bonded interactions between the tin oxalate monomer and 1,5-diaminopentane. The tin atom is four-coordinated and forms a distorted square pyramidal arrangement. The oxygen atoms are, in turn, connected to carbon atoms, completing the discrete tin oxalate unit. The tin oxalate units are anionic, and the charge compensation is achieved by the presence of the protonated amine molecule. The individual tin oxalate species are related to each other by strong hydrogen bonding with the amine molecule, completing the structure (Figure 8a,b). When viewed along the  $bc$  plane, the structure presents a zigzag chain type arrangement with the amine molecule (Figure 8a). Along the  $ab$  plane, however, the appearance is linear and more tapelike with each tin(II) oxalate unit is surrounded by four amine molecules and held in position by hydrogen bonding (Figure 8b). The Sn atoms in **III** are four-coordinated with respect to the oxygens with a Sn–O distance of 2.111 Å. The O–Sn–O bond angles are in the range 72.8–120.0° (average 90.4°). These parameters, again, agree with the literature values. The complete list of bond distances and bond angles in **III** are presented in Table 9.

### Discussion

Three new tin oxalate phases, **I**,  $[(\text{CH}_3)_2\text{NH}(\text{CH}_2)_4\text{NH}(\text{CH}_3)_2]^{2+}[\text{Sn}_2(\text{C}_2\text{O}_4)_3]^{2-}$ , **II**,  $[\text{C}(\text{NH}_2)_3]_2^+[\text{Sn}_2(\text{C}_2\text{O}_4)_3]^{2-} \cdot 2\text{H}_2\text{O}$ , and **III**,  $[\text{C}_5\text{N}_2\text{H}_{16}]^{2+}[\text{Sn}_2(\text{C}_2\text{O}_4)_3]^{2-}$ ,

have been obtained as good quality single crystals by hydrothermal synthesis. As typical of kinetically controlled solvent-mediated reactions, there is no particular correlation between the starting composition and the majority solid-phase product stoichiometry.<sup>29</sup> Although both materials involve bonding between the oxalate units and tin atoms, they exhibit distinct differences.

The oxalates **I–III** are members of a new family of inorganic framework structures synthesized by hydrothermal methods. They are obtained in the presence of structure-directing organic amines and are stabilized by multipoint hydrogen bonding. Whereas **I** has a three-dimensional architecture containing overlapping layers, **II** and **III** are formed as monomer units stabilized and held together by the amine molecules. It is observed that the structure-directing agent, *N,N,N,N*-tetramethyl-1,4-diaminobutane, used in the synthesis of **I** is disordered. While the amines are often disordered in materials prepared hydrothermally, it is rather unusual for the carbon connected to the disubstituted nitrogen alone to be disordered. Most of the earlier observations of disorder of the amine molecules related to the terminal atoms.<sup>30</sup> Recently disorder in the amine molecule involving nonterminal atoms has been observed.<sup>31</sup>

(29) Harrison, W. T. A.; Dussack, L. L.; Jacobson, A. J. *J. Solid State Chem.* **1996**, *125*, 234.

(30) Natarajan, S.; Gabriel, J.-C. P.; Cheetham, A. K. *Chem. Commun.* **1996**, 1415, and references cited therein.

(31) Bu, X.; Feng, P.; Gier, T. E.; Stucky, G. C. *J. Solid State Chem.* **1998**, *136*, 210.

(32) Zemva, H.; Jesih, A.; Templeton, D. H.; Zalkin, A.; Cheetham, A. K.; Bartlett, N. *J. Am. Chem. Soc.* **1987**, *109*, 7420. Greenwood, N. N.; Earnshaw, A. *Chemistry of the elements*; Pergamon Press: New York, 1993.

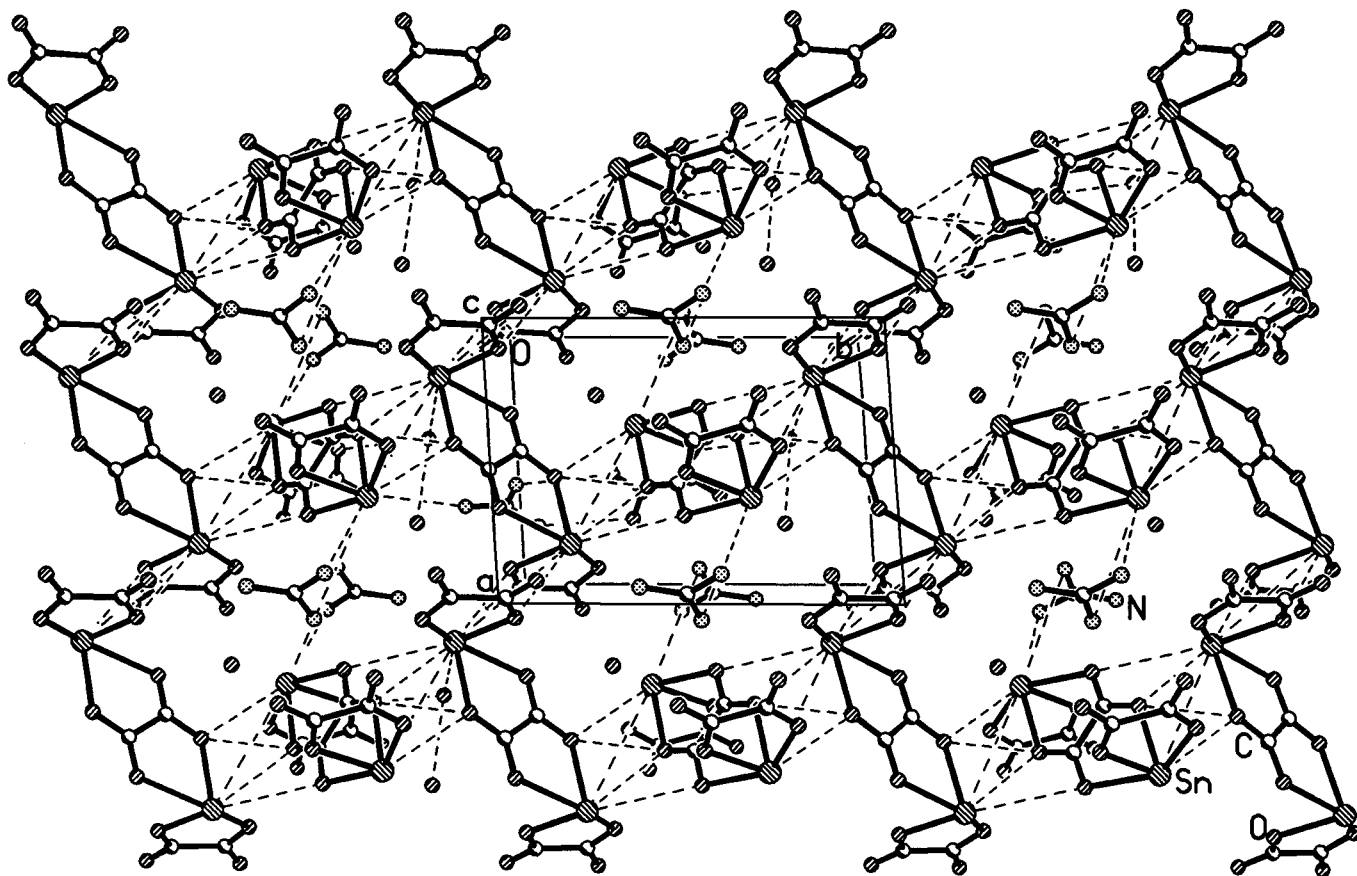


**Figure 7.** Structure of **II**,  $[\text{C}(\text{NH}_2)_3]_2^+[\text{Sn}_2(\text{C}_2\text{O}_4)_3]^{2-} \cdot 2\text{H}_2\text{O}$ , viewed along the  $c$  axis, showing the chains formed by one tin oxalate monomer. Note that the amine, water, and the other tin oxalate occupy spaces between them.

The lone pairs of the tin atoms form an important aspect of these structures. In compound **I**, the lone pairs of the neighboring Sn atoms point in opposite directions. This creates a situation wherein there is considerable interaction between the Sn atom of one layer and the lone pair of the Sn atom lying directly beneath it (Figures 2 and 3). Such an interaction enhances the inherent stability of this material. However, in the case of **II**, the lone pairs are situated in such a manner that they avoid direct interaction (Figures 5–7). This arrangement is helpful in enhancing the stability of **II**, as direct interaction between the lone pairs would have led to repulsion and lower stability. This situation is reminiscent of  $[\text{XeF}_5]^+$  type systems, where other donor groups approach the Xe atoms obliquely to avoid the lone pair.<sup>32</sup> The structure of **III** is much simpler compared to **I** and **II**. In **III**, the lone pair of electrons points toward the other monomer unit and interacts with the other tin atoms, rendering some stability to the chains.

There is no apparent structural relationship between the parent tin oxalate and compound **I**, but some comparable features exist between **II**, **III**, and the parent tin oxalate. The structure of the parent tin oxalate is made of infinite chains in which the Sn atoms and oxalate groups alternate.<sup>33</sup> In **II** and **III**, however, such infinite chains are not present, but instead the chain length is limited to just two units (two tin atoms and one and a half oxalate units). Compounds **II** and

**III** also show some resemblance to potassium tin oxalate monohydrate  $(\text{K}_2\text{Sn}(\text{C}_2\text{O}_4)_2 \cdot \text{H}_2\text{O})$ .<sup>33</sup> In the last, the structure is made of tin oxalate monomer anions hydrogen bonded with each other through water molecules. We see similar features in **II**, but the interactions involve hydrogen bonding to the amine as well as water molecules. In the case of **III**, however, hydrogen bonding is only with the amine, forming a chainlike architecture. Thus, the oxalates reported in the present study represent a new class of materials where hydrogen bonding plays a crucial role in controlling both the stoichiometry and architecture.

The importance of hydrogen bonding in these materials becomes apparent when we examine the distances and angles listed in Table 10. In **I**, which has a layer structure with the organic amine at the center of a 12-membered ring, hydrogen bond interactions appear to be somewhat weaker than in **II** and **III**. This may be because **I** has a more open structure than **II** and **III**, and the stability is essentially derived from lone pair interactions between the layers (and marginally from the amine molecules situated between the layers). Compounds **II** and **III**, on the other hand, show a clear dominance of hydrogen bonding with donor–acceptor ( $\text{O} \cdots \text{H}$ ) distances in the range 1.98–2.54 Å and the majority of the angles above 150° ( $\text{O} \cdots \text{H} - \text{N}$ ). Hydrogen bonding in **II** also involves the water molecules. Since the angles between the various donor and acceptor sites in **II** are above 150°, we obtain a situation where the water, the amine, and the inorganic oxalate monomers form a sheetlike architecture in **II** (Figure 6). In the case

(33) Christie, D.; Howie, R. A.; Moser, W. *Inorg. Chim. Acta* **1979**, *36*, L447.



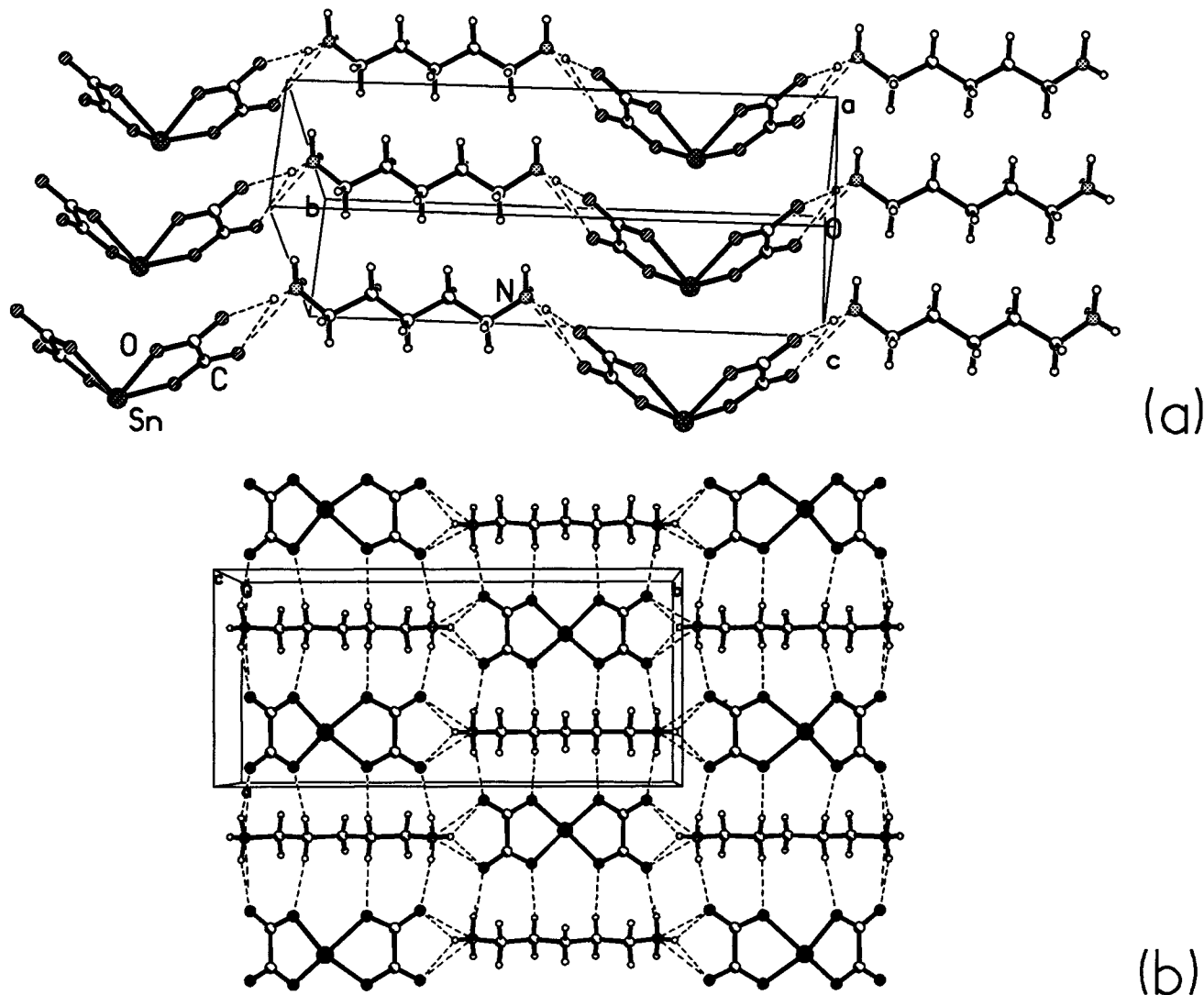


**Figure 8.** (a) Structure of **III**,  $[\text{C}_5\text{N}_2\text{H}_{16}]^{2+}[\text{Sn}_2(\text{C}_2\text{O}_4)_3]^{2-}$ , viewed along the  $bc$  plane, showing the zig zag chainlike nature of the structure (b) Structure of **III** viewed along the  $ab$  plane, showing the tapelike arrangement between the monomer and the protonated amine.

of **III**, the amine and the monomer form a linear chain or tapelike architecture (Figure 8). The ideal angle for a planar architecture is  $180^\circ$ . Thus, **I–III** constitute examples of open-framework structures where multi-point hydrogen bonding contributes to the stability.

It is interesting to compare the coordination environment of  $\text{Sn}^{\text{II}}$  atoms in the phosphates and the oxalates. Most of the earlier tin(II) phosphates<sup>34–37</sup> essentially have three- or four-coordination, forming a trigonal pyramidal  $\text{SnO}_3$  or distorted square pyramidal  $\text{SnO}_4$  moieties as the building units. In the present system, the tin(II) oxalates have higher coordination numbers ranging from 4 and 6 ( $\text{SnO}_4$  or  $\text{SnO}_6$ ). This, we believe, is because the average charge per oxygen on the oxalate (0.5) is less than that on the phosphate (0.75), such that more oxalate oxygens are needed to satisfy the valence of tin.

Thermogravimetric analysis (TGA) of **I–III** was carried out in static air from room temperature to  $900^\circ\text{C}$ . Compounds **I** and **III** show a single sharp mass loss of about 50% of the total mass of the sample, in the region  $280\text{--}300^\circ\text{C}$  for **I** and in the region  $220\text{--}280^\circ\text{C}$  for **III**. This corresponds to the loss of carbon from the oxalate unit as well as the amine molecules from the material (calculated 54% for **I** and 51% for **III**). For compound **II**, the results indicate three distinct steps. A mass loss of 5% occurring at  $200^\circ\text{C}$  corresponds to the loss of water (calculated 5.1%), the loss of 6% in the region  $260\text{--}360^\circ\text{C}$  corresponds to the loss of the amine (calculated 8.5%), and a sharp loss of 7.5% in the range  $360\text{--}390^\circ\text{C}$  corresponds to the loss of carbon (calculated 10%) from the oxalate unit. In all of the cases, the decomposed samples were poorly crystalline as found by powder X-ray diffraction, with the XRD lines corresponding to crystalline phase  $\text{SnO}$  (JCPDS: 13–111).

The oxalates **I–III** were synthesized by a careful adjustment of the pH of the synthesis mixture (different phases are formed at lower pH<sup>36,37</sup>). Since the synthesis of all three were effected at near neutral pH, we believe that the phosphoric acid in the initial synthesis mixture essentially acts as a mineralizer, similar to  $\text{F}^-$  ions in

(34) Natarajan, S.; Cheetham, A. K. *Angew. Chem., Int. Ed. Engl.* **1997**, *36*, 978.

(35) Natarajan, S.; Ayyappan, S.; Cheetham, A. K.; Rao, C. N. R. *Chem. Mater.* **1998**, *10*, 1627.

(36) Natarajan, S.; Cheetham, A. K. *Chem. Commun.* **1997**, 1089; *J. Solid State Chem.* **1997**, *134*, 207.

(37) Ayyappan, S.; Bu, X.; Cheetham, A. K.; Rao, C. N. R. *Chem. Commun.*, in press.

**Table 10. Important Hydrogen Bond Distances and Angles in Compounds I–III**

moiety	distance (Å)	moiety	angle (deg)
<b>Compound I</b>			
O(3)–H(2)	2.849(5)	O(3)–H(2)–C(2)	143.9(1)
O(6)–H(3)	2.043(3)	O(6)–H(3)–C(2)	133.4(1)
O(5)–H(4)	2.575(6)	O(5)–H(4)–C(2A)	135.2(9)
O(5)–H(5)	2.231(5)	O(5)–H(5)–C(2A)	167.5(7)
O(2)–H(8)	2.671(4)	O(2)–H(8)–C(4)	123.1(3)
O(1)–H(10)	2.748(2)	O(1)–H(10)–C(5)	154.5(5)
O(5)–H(12)	2.517(2)	O(5)–H(12)–C(5)	159.0(9)
<b>Compound II</b>			
O(9)–H(1)	2.439(1)	O(9)–H(1)–N(11)	139.8(2)
O(10)–H(1)	2.291(7)	O(10)–H(1)–N(11)	147.7(6)
O(11)–H(2)	2.101(7)	O(11)–H(2)–N(11)	169.1(4)
O(200)–H(3)	2.190(8)	O(200)–H(3)–N(12)	157.1(9)
O(5)–H(4)	2.080(1)	O(5)–H(4)–N(12)	165.3(5)
O(9)–H(5)	2.030(9)	O(9)–H(5)–N(13)	157.3(1)
O(12)–H(6)	2.341(7)	O(12)–H(6)–N(13)	129.0(1)
O(200)–H(6)	2.538(6)	O(200)–H(6)–N(13)	143.0(3)
O(12)–H(7)	2.167(9)	O(12)–H(7)–N(21)	154.1(9)
O(9)–H(8)	2.133(7)	O(9)–H(8)–N(21)	168.6(6)
O(10)–H(9)	2.342(3)	O(10)–H(9)–N(22)	133.7(5)
O(11)–H(10)	1.984(2)	O(11)–H(10)–N(22)	167.6(7)
O(100)–H(11)	2.199(9)	O(100)–H(11)–N(23)	160.0(2)
O(3)–H(12)	2.116(2)	O(3)–H(12)–N(23)	167.6(9)
<b>Compound III</b>			
N(1)–H(1)	2.021(1)	O(2)–H(1)–N(1)	147.9(2)
N(1)–H(2)	2.293(2)	O(2)–H(2)–N(1)	140.0(1)
C(1)–H(3)	2.588(3)	O(1)–H(3)–C(1)	149.9(9)
C(2)–H(4)	2.554(6)	O(1)–H(4)–C(2)	175.0(2)

some of the phosphate-based open-framework materials reported in the literature,<sup>38,39</sup> rather than form part of the framework (the synthesis of phosphate framework materials is generally carried out under acidic conditions). It would be worthwhile exploring the effect of HCl

(38) Chippindale, A. M.; Natarajan, S.; Thomas, J. M.; Jones, R. H. *J. Solid State Chem.* **1994**, *111*, 18.

(39) Guth, J. L.; Kessler, H.; Wey, R. *Stud. Surf. Sci. Catal.* **1986**, *28*, 121. Férey, G. *J. Fluorine Chem.* **1995**, *72*, 187.

or other additives on the oxalate structures obtained by the hydrothermal technique. The oxalates **I–III** reported in this study along with the previously known tin(II) phosphate and organophosphonate materials illustrate the profound influence of the reaction conditions on the composition and structure of the products obtained hydrothermally. While it is evident that the Sn(II) lone pair has considerable stereochemical consequences, the exploitation of this unit in a structure-directing role, especially in the presence of other organic structure-directing agents, requires further evaluation.

## Conclusions

The present study shows that a new class of open-framework tin(II) oxalates are obtained when the synthesis is carried out in the presence of structure-directing amines. The open-framework tin(II) phosphates are found in four structure classes: monomers, chains, sheets, and 3-D types. In the present investigation of the tin(II) oxalates, we have found a monomer and a sheet architecture. It is noteworthy that one of the oxalates in the present study has an unusual coordination for Sn resembling the classic 14 electron systems such as  $[\text{IF}_6]^-$ . The unique coordination environment of Sn(II) as well as the Sn(II) oxalate–amine structures described here suggest that it would be profitable to explore this lead further by investigating other tin(II) dicarboxylates synthesized under similar conditions. Dicarboxylates of other metals are also likely to yield interesting coordination environments and new open-framework structures.

**Acknowledgment.** The authors thank Unilever plc for providing a research grant in support of our UCSB–JNCASR joint program.

CM980574R